Sensitization of knee-innervating sensory neurons by tumor necrosis factor-α activated fibroblast-like synoviocytes: an in vitro, co-culture model of inflammatory pain.

Sampurna Chakrabarti, Luke A. Pattison, Charity N. Bhebhe, Gerard Callejo, David C. Bulmer, Ewan St. John Smith.

Department of Pharmacology, University of Cambridge.

Corresponding author: Ewan St. John Smith

Department of Pharmacology, University of Cambridge

Tennis Court Road, Cambridge CB2 1PD.

Email: es336@cam.ac.uk

Keywords: synoviocytes, sensory neurons, pain, inflammation, tumor necrosis factor, complete Freund's adjuvant, knee

Abbreviations:

FB = Fast Blue, FLS = Fibroblast-like synoviocyte, IL = Interleukin, PG = Prostaglandin, COX = Cyclooxygenase, knee neurons = knee-innervating dorsal root ganglion neurons, CFA = Complete Freund's adjuvant, CDH = Cadherin, CD = Cluster of differentiation, P = Passage, RT-PCR = Reverse transcription – polymerase chain reaction, DRG = Dorsal root ganglion, RA = Rheumatoid arthritis, OA = Osteoarthritis, MLS = Macrophage-like synoviocyte, MMP = Matrix metalloprotease, VCAM = Vascular cell adhesion molecule, TNF = Tumor necrosis factor, AIA = Antigen-induced arthritis, TRP = Transient receptor potential, ASIC = Acid-sensing ion channel, CGRP = Calcitonin gene-related peptide, ECS = Extracellular solution, PBS = Phosphate-buffered saline, Ipsi = CFA-injected side, Contra = Non-injected knee, RNA = Ribonucleic acid, DNA = Deoxyribonucleic acid, L = Lumbar, KC = Keratinocyte chemoattractant, ANOVA = Analysis of variance, AP = Action potential, RMP = Resting membrane potential, AHP = Afterhyperpolarization, HPD = Half peak duration, LIX = Lipopolysaccharide induced chemokine, MCP = Monocyte chemoattractant protein, MCSF = Macrophage colony stimulating factor, MIG = Monokine induced by gamma interferon, MIP = Macrophage inflammatory protein, RANTES = Regulated on activation, normal T-cell expressed and secreted, SDF= Stromal cell derived factor, GM-CSF = Granulocyte-macrophage colony stimulating factor, GPCR = G protein-coupled receptors.

Abstract (350 words)

Background:

Pain is a principle contributor to the global burden of arthritis with peripheral sensitization being a major cause of arthritis-related pain. Within the knee joint, distal endings of dorsal root ganglion neurons (knee neurons) interact with fibroblast-like synoviocytes (FLS) and the inflammatory mediators they secrete, which are thought to promote peripheral sensitization. Therefore, we investigated the communication between knee neurons and FLS in a co-culture system.

Methods:

Inflammation in FLS (isolated from mouse patella) was induced by stimulation with tumor necrosis factor-α (TNF-FLS). Expression of relevant genes, secretion of cytokines and functional acid response was assessed using polymerase chain reactions, inflammatory antibody array blots and Ca^{2+} imaging respectively. Electrophysiology was performed on dissociated knee neurons in mono-culture, co-culture with control FLS or TNF-FLS, or supernatant derived from TNF-FLS cultures to determine electrical excitability and sensitivity to transient receptor potential (TRP) agonists. Two group comparisons were conducted using Student's t-tests (distributed variable) or chi-sq tests (categorical variable). ANOVA followed by Tukey's post-hoc test was performed for comparing more than two groups.

Results:

Compared to control, TNF-FLS showed increased expression of interleukin-6 (*Il-6*, $p < 0.01$, unpaired t-test) and *Il-1r1* ($p < 0.05$, unpaired t-test), and enhanced cytokine secretion. FLS also responded to acidic stimuli and the percentage of TNF-FLS acid responders increased in the pH range 6.0-5.0 ($p < 0.001$, chi-sq test). Co-culture of DRG neurons with TNF-FLS or supernatant

derived from TNF-FLS depolarized the resting membrane potential ($p < 0.01$, ANOVA), increased spontaneous action potential firing ($p < 0.05$, ANOVA) and enhanced TRPV1 function ($p < 0.05$, ANOVA) of knee neurons consistent with a role for FLS in the sensitization of pain sensing nerves in arthritis.

Conclusions:

TNF-FLS have a pro-nociceptive phenotype, displaying enhanced acid sensitivity and increased secretion of pro-inflammatory cytokines. Co-culture with TNF-FLS or supernatant from TNF-FLS, induces hyperexcitability of knee neurons and enhances TRPV1 function. Data from this study demonstrate the ability of FLS activated by TNF-α to promote neuronal sensitization, results that highlight the importance of both non-neuronal and neuronal cells to the development of pain in arthritis.

Background

Joint inflammation and pain are the major clinical symptoms of arthritis. Inflammation is part of the body's immune response to tissue damage and involves multiple cell types, including lymphocytes and synoviocytes. These non-neuronal cells are either in direct contact with, or in close proximity to, the distal endings of dorsal root ganglion (DRG) sensory neurons that innervate the joints. The physical interaction of sensory neurons with non-neuronal cells and the mediators they secrete, is thought to cause peripheral sensitization of knee-innervating nerves, which is a key pathology in the development of inflammatory pain.

The knee is a richly innervated, diarthrodial joint that is lined by the synovial membrane, which is composed of synoviocytes in its intimal lining layer and lymphocytes in its sub-lining layer (1). During inflammatory diseases such as rheumatoid arthritis (RA), the joint undergoes hyperplasia due to T lymphocyte infiltration and fibroblast-like synoviocyte (FLS) proliferation. FLS are key effector cells in RA as they become active upon stimulation by inflammatory cytokines (released by macrophage-like synoviocytes, MLS, and T-cells) and secrete matrix metalloproteases (MMP) that cause joint destruction (2). In addition, FLS can also support and maintain the ongoing inflammation in arthritic joints by themselves secreting pro-inflammatory mediators (2). Building on this, recent single-cell transcriptional analysis of patient-derived RA-FLS, and their subsequent transfer into mouse knee joints, has identified distinct FLS subgroups: "destructive" and "inflammatory" (3). Furthermore, deletion of cadherin-11 (CDH-11), a key surface marker of FLS, causes hypoplasticity in murine joints and makes them resistant to inflammatory arthritis (4), evidence further supporting a critical role of FLS in arthritic pathology.

FLS derived from rodent and human joints proliferate in vitro, unlike MLS, enabling their extensive characterization (1). Interestingly, human RA-FLS are shown to be "imprinted

107 aggressors" that retain inflammatory phenotype over several passages, although the effect of these
108 activated FLS on sensory neurons remains largely unexplored (1,5). In rodents, it has been reported
109 that FLS derived from K/BxN mice (a spontaneous, chronic arthritis model) (5) and supernatants
110 from cultured FLS derived 3-days after induction of antigen-induced arthritis (AIA) in rats (6)
111 have increased levels of secreted cytokines compared to control FLS. Several other studies have
112 utilized interleukin 1β (IL-1β) or tumor necrosis factor-α (TNF-α) stimulation to robustly induce
113 an inflammatory phenotype in FLS (7–10). In this study we tested two modes of FLS activation to
114 understand their inflammatory phenotype. Firstly, we tested for pro-inflammatory phenotype in
115 FLS derived from mice undergoing the commonly used acute, unilateral complete Freund's
116 adjuvant (CFA) model, which, as previously reported, can produce robust knee inflammation, knee
117 neuron hyperexcitability and a concomitant decrease in digging behavior (11). Secondly, we tested
118 TNF-α (a cytokine that is upregulated in tissues derived CFA-injected mice (12)) stimulated FLS
119 derived from mouse knee, and determined their inflammatory phenotype to understand the
120 potential of activated FLS to induce sensitization of sensory neurons.

121

122 Since arthritic FLS reside in a pro-inflammatory environment which is often (13) (but not always
123 (14)) acidic, it is perhaps unsurprising that they express algogen sensing ion channels including
124 proton sensors (15,16) and various transient receptor potential (TRP) channels (17), such as
125 TRPV1 (transducer of noxious heat and low pH) and TRPA1 and TRPM8 (cold transducers).
126 Experiments conducted on SW982, a human tumor derived synoviocyte cell line, and primary FLS
127 from an RA patient, have demonstrated that a Ca^{2+} influx occurs upon application of the TRPV1
128 agonist capsaicin in an acidic (pH 7.1) environment and upon application of the TRPA1 and
129 TRPM8 agonist icilin (18). In addition to *Trpv1*, the human FLS cell lines SW982 and MH7A also

130 express *Trpv4* (warmth and tonicity transducer), and both *Trpv1* and *Trpv4* are upregulated by
131 TNF-α stimulation (19,20). Since most of these experiments were conducted on immortalized cell
132 lines, which thus might not be physiologically relevant, there is a need to investigate TRP channel
133 function in primary FLS. By contrast, acid sensors have been better studied in FLS derived from
134 mouse joints, leading to the identification of acid-sensing ion channel 3 (ASIC3) as a major proton
135 transducer. FLS from wild-type mice cultured in IL-1β show increased intracellular Ca^{2+} influx
136 and cell death in response to acid compared to FLS derived from $ASIC3^{-/-}$ mice, suggesting a
137 physiological role of ASIC3 and acid-sensing in general in FLS (16,21,22). Therefore, in this study
138 we sought to compare the algogen sensitivity of FLS before and after inducing an inflammatory
139 phenotype using Ca^{2+} imaging.

140 Given the complex interaction of cells in the joint environment, co-culture has proved to be an
141 important tool for dissecting FLS biology. Co-culture of human RA-FLS with T-cells (23–26) or
142 macrophages/monocytes (27–29) increased the concentration of prostaglandin (PG) E_2, IL-6, IL-
143 8, MMP-1 and MMP-3 in the culture medium, along with increased expression of adhesion
144 molecules such as vascular cell-adhesion molecule (*Vcam-1*) on FLS in a cell-mediated and
145 soluble-factor mediated manner. Furthermore, upregulation of these pro-inflammatory mediators
146 in culture supernatants was inhibited by anti-TNF-α (26,30) and anti-IL-6 antibodies (30).
147 Additionally, IL-15 secreted from human RA-FLS promotes survival of B-cells (31) and natural
148 killer cells (32) in co-culture, further demonstrating the importance of FLS in maintaining the
149 proinflammatory environment of arthritic joints. Although co-culture techniques have revealed
150 multiple immune interactions within the joint environment, the communication between neurons
151 and non-neuronal cells is less well understood in the context of knee inflammation. Culturing DRG
152 neurons with FLS derived from chronic AIA rats increased expression of receptors associated with

153 nociception, namely neurokinin 1, bradykinin 2 and TRPV1 in neurons (6), validating the premise
154 of co-culture studies to understand neuron-synoviocyte communication within the arthritic joint.
155 However, these studies did not functionally assess modulation of DRG neuron excitability, which
156 is a key mechanism of peripheral sensitization and hence pain. We recently showed that human
157 osteoarthritic (OA) synovial fluid (a lubricating fluid largely secreted by FLS (1)) can cause
158 hyperexcitability of murine sensory neurons and increase TRPV1 function (33). Therefore, in this
159 study, we hypothesized that after induction of inflammation, mouse knee-derived FLS will
160 increase excitability and TRP function of knee-innervating DRG neurons (knee neurons) in an
161 FLS-DRG neuron co-culture system.

162

163

164

165

166

167

168

169

170

171

172

173 **Methods**

174 Animals

175

176 All mice used in this study were 6-12 week old C57BL/6J mice (Envigo). Unless otherwise stated,
177 female mice were used since in humans, females are at a higher risk for inflammatory pain (34).
178 Mice were housed in groups of up to 5 in a temperature controlled (21 °C) room with appropriate
179 bedding materials, a red shelter and enrichment. They were on a 12-hour/light dark cycle with food
180 and water available *ad libitum*. Experiments in this study were regulated under the Animals
181 (Scientific Procedure) Act 1986, Amendment Regulations 2012. All protocols were approved by
182 a UK Home Office project license granted to Dr Ewan St. John Smith (P7EBFC1B1) and reviewed
183 by the University of Cambridge Animal Welfare and Ethical Review Body.

184

185 Knee injections

186

187 Under anesthesia (100 mg/kg ketamine and 10 mg/kg xylazine, intra-peritoneally) mice were
188 injected intra-articularly through the patellar tendon into each knee with the retrograde tracer, fast
189 blue (FB, 1.5 μl 2% in 0.9% saline, Polysciences) or into the left knee with 7.5 μl CFA (10 mg/ml,
190 Chondrex). Vernier's calipers were used to measure knee width (as before (11)) pre- and 24-hour
191 post-CFA injection.

192

193 Isolation and culture of FLS

194

195 24-hour after CFA injection into the knee, mice were killed by cervical dislocation and
196 decapitation. Knee joints were exposed by removing the skin, then the quadriceps muscles were
197 resected in the middle and pulled distally to expose the patellae. Patellae were then collected by
198 cutting through the surrounding ligaments, as described before (35), in phosphate-buffered saline
199 (PBS) and then transferred into one well of a 24-well plate with FLS culture media containing:
200 Dulbecco's Modified Eagle Medium F-12 Nutrient Mixture (Ham) (Life Technologies), 25% fetal
201 bovine serum (Sigma), 2 mM glutamine (Sigma) and 100 mg/ml penicillin/streptomycin (Life
202 Technologies). Cells took approximately 10 days to grow to 70% confluency; medium was
203 changed every other day. For P1, FLS were trypsinized with 1% trypsin (Sigma), re-suspended in
204 FLS culture media and transferred into two wells of a 6-well plate. FLS from two animals were
205 combined at P2. For subsequent passages, FLS were transferred into 60 mm dishes. Contralateral
206 (Contra) and CFA-injected knees/cells (Ipsi) were kept separate at all stages. The cells were
207 maintained in a humidified, 37 °C, 5% CO_2 incubator. FLS were also cultured until P5 from mice
208 that had not undergone any knee CFA injection (control). A random selection of these dishes, from
209 three separate biological replicates, was incubated for 24 to 48-hours (as per experimental design)
210 in culture medium with recombinant mouse TNF-α (10 ng/ml from a stock solution of 100 μg/ml
211 made up in 0.2 % bovine serum albumin and sterile PBS, R&D systems, aa-80325) to stimulate
212 release of inflammatory mediators (TNF-FLS) (5).

213

214 Culture of Raw 264.7 cells

215

216 Raw 264.7 cells (EACC) were cultured in medium containing Dulbecco's Modified Eagle Medium
217 F-12 Nutrient Mixture (Ham) (Life Technologies), 10% fetal bovine serum (Sigma), 2 mM
218 glutamine (Sigma) and 100 mg/ml penicillin/streptomycin (Life Technologies). Cells were
219 maintained in a humidified 37 °C, 5% CO_2 incubator.

220

221 RNA extraction and reverse transcriptase – quantitative/ polymerase chain reaction (RT-q/PCR)

222

223 For all conditions, RNA was extracted from two 60 mm dishes (Thermo Fisher) of FLS (various
224 passages) and from one T-25 flask (Greiner Bio-one) of Raw 264.7 cells at P3 using the RNeasy
225 Mini Kit (Qiagen). 500 ng of the extracted RNA was used to synthesize cDNA using a High
226 Capacity cDNA RT kit (Applied Biosystems) following the manufacturer's guidelines, using a
227 T100 Thermal Cycler (Bio-Rad). The resultant cDNA was diluted to a 1:5 ratio with nuclease free
228 water and quantitative PCR (qPCR) was performed using a StepOnePlus Real Time PCR system,
229 following the manufacturer's guidelines on settings (Applied Biosystems) using TaqMan probes
230 (Thermo Fisher) (See Supplementary Table 1 in Additional File 1). The fluorescence intensity of
231 samples was captured during the last minute of each cycle. All reactions were run in triplicate with
232 appropriate negative controls with water containing no cDNA.

233 For qPCR reactions, data were obtained as Ct values (the cycle number at which fluorescent signals
234 emitted by the TaqMan probe crossed a threshold value). Only Ct values below 35 were analyzed
235 to determine ΔCt values by subtracting the Ct of *18S* ribosomal RNA from the Ct of target gene
236 (36). ΔCt values of target genes were subtracted from average ΔCt values of their controls to
237 calculate ΔΔCt, followed by 2^(- ΔΔCt) to calculate fold change (37).

238 FLS gene expression was also assessed by RT-PCR. DreamTaq Polymerase (Thermo Fisher) was
239 used to amplify a section within the open reading frames of various genes from 5 ng template
240 cDNA. The sequences of designed oligonucleotides (Sigma) are listed in Supplementary Table 1
241 in Additional File 1. Negative controls (using water/RNA as the template) were performed for
242 each biological sample with a randomly selected primer pairing. PCR products were resolved on
243 2% agarose containing 1X GelRed Nucleic Acid Stain (Biotum) and imaged with a GeneFlash Gel
244 Documentation System (Syngene). A randomly selected subset of reactions was repeated with 2.5
245 ng template cDNA to ensure reproducibility. Densitometry analyses were performed using ImageJ
246 Software (NIH) where relative expression was determined by dividing the band intensity of each
247 gene by that of the housekeeping gene, *18S* ribosomal RNA, for each biological replicate.

248

249 Cytokine antibody array

250

251 Before RNA extraction, 2 ml of culture media from P5 Contra, Ipsi, control and TNF-FLS (48-
252 hour) were collected and stored at -80 °C until use. Culture medium was pooled from three cultures
253 for each of the four conditions and assayed (undiluted) for the presence of 40 inflammatory
254 mediators using Mouse Inflammatory Antibody Array Membranes (ab133999, Abcam) according
255 to the manufacturer's instructions. Chemiluminescence was imaged using a BioSpectrum 810
256 imaging system (UVP) with 3 min exposure. Location of the 40 cytokines detected by the array
257 membranes are shown in Supplementary Table 2 in Additional file 1.

258 Densitometry of the spots in the array membranes was performed using ImageJ software (NIH).
259 Briefly, the mean gray value of each spot was measured from all membranes using the same

260 circular region of interest. The spots of interests were then background (average of all negative
261 control spots) subtracted and normalized to the positive control spots of the reference membrane
262 (control FLS media). Fold change was obtained by dividing normalized intensities of the
263 membrane of interest and the control membrane, analyte-by-analyte.

264

265 DRG neuron isolation and culture

266

267 Lumbar DRG (L2-L5, those that primarily innervate the knee) were collected from FB labelled
268 mice 7-10 days after knee injections in ice cold dissociation media containing L-15 Medium (1X)
269 + GlutaMAX-l (Life Technologies), supplemented with 24 mM $NaHCO_3$. DRG were then
270 enzymatically digested in type 1A collagenase (Sigma) and trypsin solution (Sigma) at 37 °C,
271 followed by mechanical trituration as described before (11). Dissociated DRG neurons were plated
272 onto poly-D-lysine and laminin coated glass bottomed dishes (MatTek, P35GC-1.5-14-C) and
273 cultured either on their own (mono-culture), on a layer of FLS (co-culture, see below) or in 48-
274 hour conditioned media from TNF-FLS for 24-hours. The DRG culture medium contained L-15
275 Medium (1X) + GlutaMAX-l, 10% (v/v) fetal bovine serum, 24 mM $NaHCO_3$, 38 mM glucose,
276 2% (v/v) penicillin/streptomycin.

277

278 DRG neuron/FLS co-culture

279

280 For co-culture studies, FLS were plated onto MatTek dishes and cultured for 24-hours with FLS
281 culture media (with or without TNF-α stimulation). The next day medium was removed from FLS
282 plates, then DRG neurons were isolated as described above and plated on top of the FLS. Co-
283 culture plates were then kept in DRG culture medium for up to 24-hours for electrophysiogical
284 recording.
285
286 Cell staining

287 **FLS immunocytochemistry:** FLS were plated overnight in wells of a 24-well plate, fixed with
288 Zamboni's fixative (38) for 10 min, permeabilized with 0.05 % TritonX-100 and blocked with
289 antibody diluent (0.2% (v/v) Triton X-100, 5% (v/v) donkey serum and 1% (v/v) bovine serum
290 albumin in PBS) for 30 min. The cells were then incubated overnight at 4 °C in 1:100 (in antibody
291 diluent) anti-cadherin-11 antibody (CDH-11, rabbit polyclonal, Thermo Fisher, 71-7600). Cells
292 were washed three times with PBS-tween and incubated in the conjugated secondary antibody,
293 anti-rabbit Alexa-568 (1:1000 in PBS, Thermo Fisher, A10042) for 1-hour at room temperature
294 (21 °C). The secondary antibody was washed off three times with PBS-tween and the cells were
295 incubated in the nuclear dye DAPI (1:1000 in PBS, Sigma, D9452) for 10 min. Cells were further
296 washed with PBS-tween once and imaged in PBS using an EVOS FLoid Cell Imaging Station
297 (Thermo Fisher) at 598 nm (for CDH-11) and 350 nm (for DAPI) wavelength of light. Cells
298 without primary antibody did not show fluorescence.

299 **DRG/FLS co-culture live cell stain:** To visualize neuron/FLS co-culture, live cell imaging was
300 performed. FLS were plated on MatTek dishes with 1:1000 (diluted in FLS culture medium)
301 CellTracker Deep Red Dye (Thermo Fisher, C34565) and incubated for 24-hours in a humidified
302 37 °C, 5% CO_2 incubator. Dissociated DRG neurons (see above) were incubated in CellTracker

303 Green Dye (1: 1000 diluted in DRG culture media, Thermo Fisher, C7025) for 15 min at room
304 temperature (21 °C), centrifuged (16000 g, 3 min, 5415R, Eppendorf) and re-suspended in fresh
305 medium. The FLS dishes were then washed twice with PBS and the neuronal suspension was
306 plated on top of the FLS monolayer and incubated overnight in the incubator. The co-culture dishes
307 were washed with PBS and imaged the following day using an Olympus BX51 microscope and
308 QImaging camera at 650 nm (for deep red dye) and 488 nm (for green dye) wavelength of light.

309

310 Whole-cell patch-clamp electrophysiology

311 Neurons were bathed in extracellular solution containing (ECS, in mM): NaCl (140), KCl (4),
312 $MgCl_2$ (1), $CaCl_2$ (2), glucose (4) and HEPES (10) adjusted to pH 7.4 with NaOH. Only FB
313 labelled neurons identified by their fluorescence upon excitation with a 365 nm LED (Cairn
314 Research) were recorded. Patch pipettes of 5–10 MΩ were pulled with a P-97 Flaming/Brown
315 puller (Sutter Instruments) from borosilicate glass capillaries and the intracellular solution used
316 contained (in mM): KCl (110), NaCl (10), $MgCl_2$ (1), EGTA (1), HEPES (10), Na_2ATP (2),
317 Na_2GTP (0.5) adjusted to pH 7.3 with KOH.

318 Action potentials (AP) were recorded in current clamp mode without current injection (to
319 investigate spontaneous AP firing) or after step-wise injection of 80 ms current pulses from 0 –
320 1050 pA in 50 pA steps using a HEKA EPC-10 amplifier (Lambrecht) and the corresponding
321 Patchmaster software. AP properties were analyzed using Fitmaster software (HEKA) or IgorPro
322 software (Wavemetrics) as described before (11) and shown in Figure 3D (inset). Neurons were
323 excluded from analysis if they did not fire an AP in response to current injection. For recording
324 whole-cell voltage-clamp currents in response to TRP agonists capsaicin (1 μM from a 1 mM stock

325 in ethanol, Sigma-Aldrich), cinnamaldehyde (100 μM from a 1 M stock in ethanol, Alfa Aesar)
326 and menthol (100 μM from a 1 M stock in ethanol, Alfa Aesar), a 5 s baseline was established
327 with ECS, followed by a 5 s randomized drug application. Peak drug response was measured in
328 Fitmaster by subtracting the average of 2 s baseline immediately preceding the drug application
329 and the maximum peak response reached during the 5 s of drug application. Peak current density
330 is represented in graphs by dividing this peak response by the capacitance of the neuron. Data from
331 at least four mice were used in all conditions (with each mouse being used for at least two
332 conditions) and at least three neurons were recorded from each mouse in each category.

333

334 Ca^{2+} imaging

335 FLS or neurons were incubated with the Ca^{2+} indicator, Fluo-4 AM (10 μM diluted in ECS from
336 a 10 mM stock solution in DMSO, Invitrogen) for 30 min at room temperature (21 °C). Culture
337 dishes were then washed and imaged using an inverted Nikon Eclipse T*i* microscope. Fluo-4
338 fluorescence was excited using a 470 nm LED (Cairn Research) and captured with a camera (Zyla
339 cSMOS, Andor) at 1 Hz with 50 ms (for neurons) 250 ms (for FLS) exposure time using Micro-
340 Manager software (v1.4; NIH). Solutions were perfused in this system through a gravity-driven 12
341 barrel perfusion system (39). During imaging of neurons, MIP-1γ (10 and 100 ng/ml diluted in
342 ECS from a stock concentration of 0.1 mg/ml in 0.1% bovine serum albumin/sterile PBS, Sigma)
343 was applied for 20 s after establishing a baseline with ECS for 10 s. Neurons were allowed to
344 recover for 5 minutes between drug applications. 50 mM KCl was used as a positive control.

345 During imaging of FLS, a 10 s baseline was established with ECS and then pH 4-7, and TRP
346 agonists, 1 μM capsaicin, 100 μM cinnamaldehyde and 100 μM menthol were applied for 10 s

347 before a wash out period of 4 min between drug applications. TRP agonist sensitivity and acid
348 sensitivity was assessed on separate dishes. Three biological repeats were conducted on separate
349 days for each condition. 10 μM ionomycin was used as a positive control after all FLS Ca^{2+}
350 imaging experiments.

351 Analysis was conducted as described before (33). Briefly, mean grey values were extracted by
352 manually drawing around FLS or neurons in the ImageJ software. These values were then fed into
353 a custom-made R-toolbox (https://github.com/amapruns/Calcium-Imaging-Analysis-with-R.git)
354 to compute the proportion of cells responding to each drug and their corresponding magnitude of
355 response (normalized to their peak ionomycin (FLS) or KCl (neuron) response, (ΔF/Fmax); cells
356 not crossing threshold for positive controls were excluded from the analysis).

357

358 Statistics

359 Comparisons between two groups with distributed variables were performed using two-sided
360 Student's t-tests (paired if comparing two conditions of the same sample, unpaired otherwise) with
361 suitable corrections and amongst three groups using one-way analysis of variance (ANOVA)
362 followed by Tukey's post-hoc tests. Proportions were compared for categorical data using chi-sq
363 tests. Data are shown as mean ± SEM.

364

365

366

367

368

369 Results

370 1. TNF-FLS, but not FLS derived from CFA-induced inflamed knees, have a pro-
371 inflammatory phenotype and secrete cytokines that activate DRG neurons.

372 Key genes have been described that act as identifiers of cultured FLS isolated by enzymatic
373 digestion of mouse joints (5), as well as for establishing their inflammatory phenotype. In this
374 study, we performed RT-qPCR on adherent cells (P2-P5) originating from mouse patellae that
375 proliferated in culture (Figure 1A, B). From P2 to P3, the expression of the macrophage marker
376 (1,5) cluster of differentiation 68 (*Cd*-68, relative to the macrophage cell line RAW 267.4) was
377 significantly reduced, whereas the expression of FLS markers *Cdh-11* and *Cd-248* (1,5) remained
378 consistent from P2 to P5 (Supplementary Figure 1 in Additional file 1); the endothelial marker *Cd-*
379 *31* was not detected (data not shown). These results suggest that from P3, cells cultured from
380 mouse patellae were predominantly FLS and hence subsequent studies were conducted on FLS
381 from P3-P6.

382 Concurrently, to establish the pro-inflammatory phenotype of FLS, we used RT-qPCR to
383 determine the expression of the inflammatory genes *Il-6*, *Il-1r1* and *Cox-2*, as well as the
384 constitutively expressed gene *Cox-1.* When control FLS (P5) were stimulated with 10 ng/ml TNF-
385 α for 48-hours, there was an upregulation of *Il-6* (fold changes: Control, 1.5 ± 0.8 vs. TNF-FLS,
386 135.1 ± 31.1, n = 3, p = 0.006, unpaired t-test) and *Il-1r1* (fold changes: Control, 1.1 ± 0.2 vs.
387 TNF-FLS, 3.4 ± 1.0, n = 3, p = 0.04, unpaired t-test) expression levels, but not that of *Cox-2* (fold
388 changes: Control, 1.0 ± 0.2 vs. TNF-FLS, 0.8 ± 0.2, n = 3, p = 0.2, unpaired t-test) or *Cox-1* (fold
389 changes: Control, 1.0 ± 0.2 vs. TNF-FLS, 0.8 ± 0.2, n = 3, p = 0.18, unpaired t-test) (Figure 1C).

390 However, when FLS derived from the inflamed knee (Ipsi, knee width, pre-CFA, 3.1 ± 0.09 mm
391 vs. post-CFA, 4.1 ± 0.08 mm, n = 6, p = 0.0001, paired t-test, Supplementary Figure 1 in Additional
392 File 1) of CFA injected mice was compared to those of the matched contralateral knee (Contra),
393 we did not find any changes in expression levels of the genes between Contra and Ipsi FLS across
394 P2-P5 (Figure 1C, Supplementary Figure 1 in Additional File 1).

395 We next tested the media (n = 3, each) isolated from control, Contra, Ipsi and TNF-FLS against a
396 mouse inflammation antibody array (Figure 1E) to determine the levels of different secreted pro-
397 inflammatory mediators. This demonstrated that when compared to control FLS media, TNF-FLS
398 media showed presence of Regulated on activation, normal T-cell expressed and secreted
399 (RANTES) and granulocyte-macrophage colony stimulating factor (GM-CSF). Additionally,
400 TNF-FLS contained higher levels of IL-6 ($p < 0.0001$), keratinocyte chemoattractant (KC, mouse
401 homolog of IL-8, $p < 0.0001$), lipopolysaccharide induced chemokine (LIX, $p < 0.0001$), stromal
402 cell derived factor 1 (SDF-1, $p < 0.0001$), fractalkine ($p < 0.0001$), monocyte chemoattractant
403 protein 1 (MCP-1, $p < 0.0001$) and macrophage inhibitory protein 1γ (MIP-1γ, $p = 0.002$) and
404 lower levels of macrophage colony stimulating factor (MCSF, $p = 0.003$) compared to control FLS
405 media (multiple t-tests with Holm-Sidak corrections, Figure 1Dii). TNF-α was not detected in
406 TNF-FLS media as previously shown in TNF-α stimulated airway epithelial cells (40). Mirroring
407 the absence of pro-inflammatory gene upregulation in Ipsi vs. Contra FLS, the spot intensity values
408 of inflammatory cytokines between Ipsi and Contra FLS were similar (multiple t-tests with Holm-
409 Sidak corrections, graph not shown), suggesting similar levels of secreted cytokines. However,
410 when spot intensities were normalized to control FLS, TNF-FLS media showed increased levels
411 of secreted IL-6 ($p < 0.0001$, ANOVA followed by Tukey's multiple comparison test) and KC (p

412 = 0.001, ANOVA followed by Tukey's multiple comparison test) compared to Ipsi and Contra
413 FLS (Figure 1Diii).

414 Interestingly, MIP-1γ was elevated in both Ipsi and Contra FLS when compared to control and
415 TNF-FLS (Figure 1Diii), perhaps indicating its role in acute, systemic inflammatory pathways.
416 MIP-1γ has been described as having a role in hyperalgesia induced by diabetic neuropathy (41)
417 and OA-related pain (42), and we find that MIP-1γ directly activates mouse DRG neurons by
418 producing a dose-dependent Ca^{2+} influx (Supplementary Figure 1 in Additional File 1), which thus
419 might be a potential mechanism for the *in vivo* effects described above. However, because MIP-
420 1γ does not have a human homolog (NCBI gene database entry #20308), and thus has limited
421 clinical potential, we did not explore this further.

422 Taken together, our data suggest that TNF-α stimulation of FLS upregulates expression of
423 canonical inflammatory markers, whereas the *in vivo* pathology observed 24-hours after CFA-
424 induced knee inflammation does not correlate with a sustained pro-inflammatory phenotype of
425 FLS isolated from patellae of CFA mice. We also identify other soluble mediators secreted by
426 TNF-FLS that might be involved in FLS-DRG neuron communication. Therefore, given the pro-
427 inflammatory phenotype of TNF-FLS (and the lack of such phenotype in the CFA model), we
428 focused solely on the TNF-FLS for the rest of the study.

429

430 2. TNF-FLS have reduced sensitivity to mild acidosis, but enhanced sensitivity to more acidic
431 pH.

432 During arthritis, FLS are located in an environment with abundant algogens that have been shown
433 to signal through the modulation of TRP channels (2). Therefore we tested FLS sensitivity to a

434 range of acidic pH stimuli, as well as the prototypic TRP channel agonists, capsaicin (TRPV1),
435 cinnamaldehyde (TRPA1) and menthol (TRPM8) using Ca^{2+} imaging. Confirming results from
436 other studies on acid sensing in FLS (22), we found that both control and TNF-FLS respond to a
437 range of pH solutions (pH 4.0 – 7.0) with an increase in intracellular Ca^{2+} (Figure 2A, B). An
438 increased percentage of control FLS (24.1 %) respond to pH 7.0 compared to TNF-FLS (11.0 %,
439 $p = 0.0004$, chi-sq test), but in the more acidic range an increased percentage of TNF-FLS
440 responded to acid than did control FLS, i.e. pH 6.0 (control, 7.2 % vs. TNF-FLS, 26.3 %, $p <$
441 0.0001, chi-sq test) and pH 5.0 (control, 14.4 % vs. TNF-FLS, 30.5 %, $p < 0.0001$, chi-sq test).
442 At the very acidic pH of 4.0, ~ 40% ($p = 0.4$, chi-sq test) of FLS responded in both groups possibly
443 due to ceiling effect. Although the proportion of responding neurons varied, the magnitude of peak
444 normalized response was similar across the pH range in control (pH 7.0: 0.4 ± 0.04 F/Fmax (n =
445 50), pH 6.0: 0.4 ± 0.08 F/Fmax (n = 27), pH 5.0: 0.3 ± 0.03 F/Fmax (n = 46), pH 4.0: 0.3 ± 0.02
446 F/Fmax (n = 129)) and TNF-FLS (pH 7.0: 0.3 ± 0.06 F/Fmax (n = 21), pH 6.0: 0.4 ± 0.03 F/Fmax
447 (n = 50), pH 5.0: 0.3 ± 0.02 F/Fmax (n = 58), pH 4.0: 0.3 ± 0.02 F/Fmax (n = 72), Figure 2Bii).

448 To identify the proton sensors expressed by FLS that likely mediate the responses measured, we
449 conducted RT-PCR of control and TNF-FLS to determine expression of known proton-sensing G
450 protein-coupled receptors (GPCRs), ASICs and TRPV1. Our data show that FLS express the
451 proton sensing GPCRs – *Gpr4*, *Gpr65*, *Gpr68* and *Gpr132*, as well as *Asic1*, Asic*3* and *Trpv1*
452 (Figure 2Ci). When relative expression was assessed compared to the housekeeping gene *18S*,
453 *Gpr132* was found to be increased ($p = 0.005$, Figure 2Cii) in TNF-FLS implicating it as a potential
454 contributor to the enhanced proportion of acid responders seen in TNF-FLS (Figure 2Bi). The pro-
455 inflammatory phenotype of TNF-FLS was confirmed by the increased *Il-6* band intensity ($p <$

456 0.0001), as observed previously using qPCR (multiple t-tests with Holm-Sidak corrections, Figure
457 2Cii).

458 We also tested FLS sensitivity to capsaicin (control, 3/201, TNF-FLS, 13/252), cinnamaldehyde
459 (control, 1/201, TNF-FLS, 11/252) and menthol (control, 0/201, TNF-FLS, 1/194) to find that only
460 a few cells responded to each compound (data not shown). This led us to conclude that there are
461 very few mouse primary FLS with functional TRPV1 (also corroborated by the observation of low
462 *Trpv1* gene expression, Figure 2C), TRPA1 or TRPM8 ion channels and hence we did not explore
463 this further.

464 3. TNF-FLS increase knee-innervating DRG neuron excitability in co-culture.

465 Changes is primary sensory neuron excitability underlie peripheral sensitization which drives
466 arthritis-related pain (43). Non-neuronal cells like FLS, which are in close proximity with distal
467 terminals of knee neurons, can play instrumental roles in modulating sensory neuron excitability
468 by direct cell contact and/or secretion of pro-inflammatory cytokines. To determine neuron/FLS
469 communication in health and inflammation we compared the DRG neuronal excitability of four
470 groups: 1) knee neuron mono-culture, 2) knee neurons co-cultured with control FLS (Figure 3A,
471 B), 3) knee neurons with FLS that have been exposed to TNF media for 24-hour followed by DRG
472 culture media for 24-hours and 4) knee neurons with conditioned media from FLS that have been
473 exposed to TNF media for 48-hours to understand the role of soluble mediators in peripheral
474 sensitization. In current-clamp mode, we observed many neurons spontaneously firing AP in
475 groups 3 and 4. In order to statistically compare the proportions, we converted our four group data
476 into binary categories: neuron mono-culture and neuron/control FLS co-culture were assigned to
477 the class "healthy", and neuron/TNF-FLS and neuron/TNF-FLS media were assigned to the class
478 "inflamed". 19.5% of inflamed neurons (neuron/TNF-FLS, 5/21; neuron/TNF-FLS media, 3/19)

479 fired spontaneous AP compared to 2.7% (neuron mono-culture, 0/19; neuron/control FLS, 1/18)
480 of healthy neurons ($p = 0.02$, chi-sq test) suggesting that there is a general increase in excitability
481 of knee neurons when exposed to an FLS-mediated inflammatory environment (Figure 3C, D).

482 Upon measuring the AP properties (Figure 3D inset) we found that the resting membrane potential
483 (RMP) was more depolarized in the neuron/TNF-FLS media group compared to both neuronal
484 mono-culture ($p = 0.0004$) and neuron/control FLS co-culture ($p = 0.012$), which highlights that
485 secreted pro-inflammatory factors from TNF-FLS likely act upon knee neurons to increase their
486 excitability (ANOVA followed by Tukey's post hoc comparison, Figure 3Ei). The other measured
487 properties were unchanged among the four groups (ANOVA followed by Tukey's post hoc
488 comparison, Table 1, Figure 3Eii-iv).

489

490 4. TNF-FLS increase TRPV1 function and decrease TRPA1/TRPM8 function of DRG
491 neurons in co-culture.

492 DRG neurons in co-culture with inflamed FLS derived from AIA rats reportedly have increased
493 expression of TRPV1 (6). Here we sought to investigate whether FLS can modulate knee neuron
494 responses to TRP agonists using whole-cell patch-clamp recordings. Knee neurons in mono-
495 culture and when co-cultured with control FLS displayed very similar responses, i.e. a mean
496 capsaicin peak current density response of 3.5 ± 1.0 pA/pF ($n = 7$) and 3.2 ± 0.9 pA/pF ($n = 7$)
497 respectively. By contrast, knee neurons in neuron/TNF-FLS co-culture showed a trend for larger
498 magnitude of capsaicin responses (27.7 ± 9.3 pA/pF, $n = 8$), and those cultured with TNF-FLS
499 media had a capsaicin response of 65.8 ± 25.7 pA/pF ($n = 7$) which was significantly larger in
500 magnitude than neuronal mono-culture ($p = 0.02$) and neuron/control FLS co-culture ($p = 0.02$)

501 (ANOVA followed by Tukey's post-hoc comparison, Figure 4Ai,ii). No difference was observed
502 between the percentage of capsaicin responders in healthy (40.5%) vs. inflamed groups (37.5%, p
503 = 0.8, chi-sq test, Figure 4Aiii).

504 With regards to menthol (mono-culture, 2.4 ± 1.2 pA/pF, n = 7; neuron/healthy FLS, 4.8 ± 2.1
505 pA/pF, n = 6; neuron/TNF-FLS, 1.4 ± 1.2 pA/pF, n = 2; neuron/TNF-FLS conditioned media, 4.0
506 ± 1.9 pA/pF, n = 4; Figure 4Bi) and cinnamaldehyde (mono-culture, 1.9 ± 0.7 pA/pF, n = 10;
507 neuron/healthy FLS, 2.8 ± 1.1 pA/pF, n = 4; neuron/TNF-FLS, 0.6 ± 0.3 pA/pF, n = 3,
508 neuron/TNF-FLS conditioned media, 2.3 ± 1.5 pA/pF, n = 3; Figure 4Ci) responses, all four groups
509 showed similar mean peak current density values (Figure 4Bii, Cii). However, in response to both
510 the TRPA1 and TRPM8 agonists, the percentage of responding neurons was significantly less in
511 the inflamed group compared to healthy (menthol: healthy vs. inflamed, 37.8% vs. 15%, p = 0.02,
512 chi-sq test; cinnamaldehyde: healthy vs. inflamed, 43.2% vs. 15%, p = 0.006, chi-sq test, Figure
513 4Biii, Ciii). Taken together our data suggests that "inflamed" FLS can alter TRP agonist response
514 of knee neurons in co-culture.

515

516

517

518

519

520

521

522

523

524

525 Discussion

526 In this study we demonstrate that FLS can be obtained from mouse patella via cell-outgrowth and
527 maintained in culture. When stimulated with TNF-α, these FLS show an increase in: pro-
528 inflammatory gene expression, secretion of pro-inflammatory cytokines and acid sensitivity in the
529 pH 6.0-5.0 range consistent with a pro-nociceptive activated phenotype. Finally, we establish a co-
530 culture system, which shows that FLS and knee neurons can interact, specifically, factors secreted
531 by TNF-FLS increase knee neuron excitability and the magnitude of the response to capsaicin,
532 whereas the proportions of cinnamaldehyde and menthol responding neurons are diminished. To
533 the best of our knowledge, this is the first report to demonstrate FLS-mediated changes in neuronal
534 excitability in co-culture and hence directly demonstrate how FLS can regulate articular neurons
535 and in turn arthritis-related pain.

536 FLS from mouse are generally cultured by enzymatically digesting and combining excised joints
537 of fore- and hind-limbs (5,21,22,44), which assumes similarity of FLS derived from all joints.
538 However, a genome-wide study on DNA-methylation has shown that important differences exist
539 between knee and hip FLS, including of genes involved in IL-6 signaling (45). By using a cell-
540 outgrowth method to culture mouse FLS, as previously described in humans (46) and rats (6), we
541 have avoided the biological ambiguity introduced by joint-to-joint variability. Using these FLS,
542 we investigated the expression of inflammatory genes *Il-6*, *Il-1r1* and *Cox-2*, all of which have
543 been linked to the inflammatory phenotype of FLS. In brief: stimulating human-derived FLS with

544 IL-1β increases *Cox-2* and *Il-6* expression (46); increased *Il-6* expression is seen in FLS derived
545 from K/BxN mice and following 24-hour stimulation of healthy mouse FLS with TNF-α (5).
546 Lastly, supernatants from FLS derived 3-days into a rat AIA model show increased IL-6 and PGE_2
547 (6). Here we observed that neither the expression level of *Il-6*, *Il-1r1, Cox-2*, nor the level of
548 secreted cytokines were upregulated in FLS derived from CFA-injected knee. This is possibly
549 because the model used here is too brief to influence FLS gene expression. Indeed, evidence to
550 support this is that FLS derived from rats with longer (3-28 days) AIA-induced knee inflammation
551 did have higher PGE_2 and IL-6 concentrations in culture supernatants compared to control FLS
552 (6). Alternatively, the affected area of the synovium might be too small for sufficient proliferation
553 of "inflamed" FLS and thus they are lost over time in culture. This result suggests a limited role
554 of FLS in the acute CFA model of knee inflammation with regard to modulation of neuronal
555 excitability.

556 We reasoned that FLS need more direct and prolonged exposure to inflammatory mediators to
557 show a robust inflammatory phenotype. TNF-α is one such cytokine that is locally upregulated
558 within 3-hours of intra-plantar CFA injection in mice (12). It is also present in high concentrations
559 in the synovial fluid (47) and tissue of OA and RA patients (48,49); along with anti-TNF-α agents
560 being the leading treatment of RA (50). Indeed, we show that TNF-α stimulated FLS display
561 increased expression of *Il-6* and *Il-1r1* mRNA, with a concomitant increase in secretion of many
562 pro-inflammatory cytokines, including IL-6 as has been reported previously in human FLS (51).
563 This observation is consistent with the "passive responder and imprinted aggressor model" of
564 inflammatory FLS behavior (2), i.e. these cells can respond to pro-inflammatory environment and
565 then themselves become effectors to drive disease pathology. The functional repercussions of this
566 model are not well-explored and here we investigate two such possibilities: change in FLS

567 functionality after induction of inflammation and "inflamed" FLS-induced functional changes in
568 nerves supplying the knee joint to drive pain.

569 Comparing the control and TNF-FLS response to acidic stimuli, we found a decreased percentage
570 of TNF-FLS responding to pH 7.0, but in the pH 6.0-5.0 range the percentage of TNF-FLS
571 responding to acidic stimulation increased. Multiple proton-sensors with sensitivity to varied pH
572 range might underlie the apparent incongruity of TNF-FLS acid sensitivity in mild and strongly
573 acidic environment (52). For example, increased expression of proton sensors programmed to
574 detect highly acidic environments can come at the cost of sensors active at mildly acidic range.
575 This concept has been alluded to previously with mouse primary FLS showing increased *Asic3*,
576 but decreased *Asic1*, expression after IL-1β stimulation (22). The present study shows that ASIC1
577 and 3 may underlie acid sensitivity in FLS, as has been shown previously (21,22) and here we also
578 show that multiple proton sensing GPCRs are expressed in FLS. Additionally, an increased level
579 of *Gpr132* in TNF-FLS lends support to the hypothesized role of GPR132 (15) in Ca^{2+}
580 mobilization of FLS in response to acidification. Furthermore, TRPV1 is activated at pH below 6,
581 which can contribute to the enhanced acid response of TNF-FLS in that range. Although we report
582 very few FLS respond to capsaicin at physiological pH of 7.4 (as has been shown before (18)),
583 more cells responded in the TNF condition compared to control.

584 In order to understand the effector role of FLS in driving nociception through peripheral
585 sensitization, we set up a co-culture system combining FLS and knee neurons. Studying co-culture
586 of rat FLS and DRG neurons, von Banchet *et al* showed using immunohistochemistry that
587 bradykinin 2 receptor labelling (but not that of neurokinin 1 or TRPV1) was increased when DRG
588 neurons were cultured with healthy rat FLS (6), i.e. co-culture of DRG neurons with FLS can alter
589 expression of genes associated with nociception. Therefore, we first verified that knee neurons in

590 co-culture with control FLS do not show dysregulation of excitability or TRP agonist response.
591 Then we asked whether TNF-FLS modulates knee neuron function and found using whole-cell
592 patch clamp that 23% and 16% of knee neurons in neuron/TNF-FLS co-culture and neuron/TNF-
593 FLS media (inflamed conditions) respectively evoked spontaneous AP compared to 6% in
594 neuron/control FLS and 0% in neuron mono-culture (healthy conditions). This suggests that TNF-
595 FLS increases excitability of knee neurons. von Banchet *et al* (6) also showed that compared to
596 mono-culture, FLS derived from acute and chronic AIA rats induced an increase in TRPV1 protein
597 expression in DRG neurons. However, we did not see increase in proportion of neurons responding
598 to capsaicin between healthy and inflamed conditions, which might reflect a species difference
599 and/or difference in knee-specific neuronal population (unlike in this study, von Banchet *et al* did
600 not discriminate between knee-innervating neurons and non-knee innervating neurons); however,
601 we did observe that capsaicin responsive neurons produced larger magnitude responses when
602 incubated with TNF-FLS medium, see below. We also observed that cinnamaldehyde and
603 menthol-evoked responses were decreased in the inflamed condition, suggesting functional
604 downregulation of TRPA1 and TRPM8. Functional downregulation of TRPA1 might be explained
605 through desensitization via increased TRPV1 function (see below) (53) or via an increase in
606 intracellular Ca^{2+} (due to increased excitability in the inflamed condition) (54). The latter reason
607 can also be applied to explain decrease of menthol-evoked responses (55).

608 We also observed a tendency of a more depolarized RMP and an enhanced magnitude of capsaicin-
609 evoked peak current density of knee neurons in inflamed conditions, albeit both only reached
610 statistical significance in the TNF-FLS media incubated group when compared to mono-culture
611 and neuron/control FLS. These results suggest that soluble mediators released by FLS are key
612 players in modulating knee neuron excitability. We posit that because our experimental design

613 involved a media change 24-hours after TNF incubation of FLS (so as not to directly stimulate
614 neurons with residual TNF-α (56)) in the neuron/TNF-FLS co-culture condition, the accumulated
615 soluble mediator concentrations were lower compared to when knee neurons were incubated in
616 48-hours TNF-FLS conditioned media (no remaining TNF-α was measured in the media at this
617 point). Indeed we have recently established the role of soluble mediators present in OA synovial
618 fluid in increasing neuronal excitability and TRPV1 function (33). These soluble mediators mainly
619 consist of cytokines/chemokines which form complex signaling pathways with neurons (reviewed
620 in (57,58)). In this study, we have identified IL-6 (59), KC (60), RANTES (61), GM-CSF (62),
621 LIX (63), SDF-1 (61), MCP-1 (64), MIP-1γ (present study) to be upregulated in TNF-FLS media
622 which can also directly signal to neurons; and in the cases of IL-6, MCP-1 and GM-CSF increase
623 TRPV1 function (59,62,64). Although fractalkine does not directly stimulate neurons (57), a recent
624 study showed a correlation between levels of this cytokine in protein extracted from human OA
625 synovia and brain derived neurotrophic factor - tropomyosin receptor kinase B mediated signaling
626 in joint nerves to induce mechanical hyperalgesia (65).

627 Therefore, this study demonstrates an increase in knee neuron excitability and TRPV1 function
628 upon interaction with non-neuronal TNF-FLS.

629

630 **Conclusion**

631 Knee pain in arthritis is a major cause of disability and peripheral sensitization mediated by
632 enhanced excitability of nociceptive neurons play a key role in pain (43,66). Those neurons
633 supplying the knee joint are exposed to a pro-inflammatory environment due to cell-contact and
634 soluble mediator release from immune cells. One such key effector in the joint is FLS which can

respond to inflammatory mediators and also themselves secrete inflammatory soluble factors (2). In this study we show that TNF-FLS increase mRNA expression of inflammation-linked genes *Il-6* and *Il-1r1* along with enhanced secretion of cytokines compared to control. Additionally, TNF-FLS can increase excitability of knee neurons and alter TRP channel function in these neurons in a co-culture system. Therefore, we establish a direct inflammation-pain axis through FLS and DRG neurons. This system can be adapted to investigate peripheral sensitization using FLS activated by other pro-inflammatory cytokine or arthritic synovial fluid.

Declarations

Ethics approval: Mice used in this study were regulated under the Animals (Scientific Procedure) Act 1986, Amendment Regulations 2012. All protocols were reviewed by the University of Cambridge Animal Welfare and Ethical Review Body.

Consent for publication: Not applicable.

Availability of data and materials: The datasets supporting the conclusions of this article will be available in University of Cambridge Apollo Repository (https://doi.org/10.17863/CAM.44367).

Competing interests: The authors declare no competing interests.

Funding: This study was supported by Versus Arthritis Project Grants (RG 20930 and RG 21973) and Rosetrees grant (M818) to E. St. J. S. and G.C., and Crohn's and Colitis UK grant to D.C.B. (PC2019/1-Bulmer). S.C. and C.N.B were supported by Gates Cambridge Trust scholarships. L.A.P. was supported by the University of Cambridge BBSRC Doctoral Training Programme (BB/M011194/1).

Authors' contributions:

656 S.C. designed experiments, conducted experiments, analyzed data and drafted the manuscript.
657 L.A.P. and C.N.B. conducted and analyzed experiments and revised manuscript. G.C. designed
658 experiments and revised the manuscript. D.C.B revised the manuscript. E. St. J. S. designed
659 experiments and drafted the manuscript.

660 Acknowledgements:

661 The authors thank Dr Dora Lopresto (Department of Pharmacology, University of Cambridge) for
662 technical help with cell staining.

663

664

665

666

667

668

669

670

671

672

673

674

675 Figure Legends:

676

677 Figure 1: Induction of inflammation in FLS derived from mouse knee. A) Representative picture
678 showing exposed inside of the patella (black triangle) and the surrounding ligament and fat pad
679 (white triangle) after midline resection and distal pull of the quadriceps muscles. Scale bar = 2
680 mm. B) Representative picture of FLS in culture. Scale bar = 50 µm. C) Bars represent fold change
681 of the genes *Il-6*, *Il-1r1*, *Cox-2* and *Cox-1* from either Contra (vs. Ipsi) or control (vs. TNF). Black
682 hatched bars = control FLS, red bars = TNF-FLS, grey bar = Contra, white bar = Ipsi. All FLS at
683 P5. D) Images of mouse inflammatory array membranes probed against FLS conditioned medium
684 (i) which were quantified by densitometry and represented as bar graphs showing fold change of
685 various cytokines between control and TNF-FLS (ii, multiple t-test with Holm-Sidak correction)
686 and among Contra, Ipsi and TNF from control FLS media (iii, ANOVA with Tukey's post-hoc
687 test) and spot intensity differences. Dotted rectangles highlight IL-6 spots (Di) and corresponding
688 quantifications (Dii, iii). Only cytokines that were present in all of the compared groups are shown
689 in graphs. * $p < 0.05$, ** $p < 0.01$, *** $p < 0.001$ and **** $p < 0.0001$. Error bars = SEM.

690 Figure 2: Acid sensitivity in FLS. A) Representative Ca^{2+} imaging trace from an FLS responding
691 to pH 5 and ionomycin. Bi) Bars representing proportions and magnitudes (ii) of control (black
692 hatched) and TNF-FLS (red) responding to pH 7, 6, 5 and 4. Comparison between control vs. TNF-
693 FLS made using chi-sq test. Data from three biological replicates in each category. Ci) Gel image
694 of control and TNF-FLS expression of proton sensors along with the densitometry analysis of the
695 relative band intensity compared to the 18S band (ii, multiple t-test with Holm-Sidak correction).
696 ** $p < 0.01$, *** $p < 0.001$ and **** $p < 0.0001$. Error bars = SEM.

697 Figure 3: TNF-FLS mediated increase in excitability of knee neurons. A) Representative live-cell
698 imaging picture showing FLS (magenta) and neuron (cyan) in co-culture. Scale bar = 50 µm. B)
699 Representative FB labelled knee neuron (white arrow) being recorded using a patch pipette
700 (triangular shadow), surrounded by FLS (yellow arrow). Scale bar = 50 µm. C) Pie-chart showing
701 proportion of knee neurons that fired AP without current stimulation in healthy (neuron mono-
702 culture + neuron/control FLS, n = 37, black) and inflamed (neuron/TNF-FLS + neuron/TNF-FLS
703 media, n = 41, red) condition. D) Representative knee neuron incubated with TNF-FLS media
704 firing spontaneous AP along with schematic diagram of AP properties measured (inset). E) Bar
705 graphs showing measured RMP (i), threshold (ii), AHP peak (iii) and HPD (iv) from knee neurons
706 in mono-culture (n = 19, white bar/black open circle), in co-culture with control FLS (n = 18, grey
707 bar/black dotted circle), in co-culture with TNF-FLS (n = 20, light red bar/red dotted circle) and
708 incubated in TNF-FLS media (n = 21, white bar/red open circle). * $p < 0.05$ and *** $p < 0.001$,
709 ANOVA followed by Tukey's post hoc test. Data from 4-5 female mice in each group. Error bars
710 = SEM.

711 Figure 4: TNF-FLS mediated modulation of TRP agonist response in knee neurons. Representative
712 traces showing capsaicin (TRPV1 agonist, Ai), cinnamaldehyde (TRPA1 agonist, Bi) and
713 menthol- (TRPM8 agonist, Ci) evoked responses in knee neurons. Black traces obtained from knee
714 neuron in mono-culture, red trace obtained from knee neuron incubated in TNF-FLS media. White
715 boxes represent perfusion of extracellular solution. Bar graphs showing peak current densities of
716 capsaicin- (Aii), cinnamaldehyde- (Bii) or menthol-evoked (Cii) currents from knee neurons in
717 mono-culture (white bar/black open circle), in co-culture with control FLS (grey bar/black dotted
718 circle), in co-culture with TNF-FLS (light red bar/red dotted circle) and incubated in TNF-FLS
719 media (white bar/red open circle) Comparison between groups made using ANOVA with Tukey's

post hoc test. Bar graphs showing percent of knee neurons that responded to capsaicin (Aiii), cinnamaldehyde (Biii) and menthol (Ciii) in healthy (neuron mono-culture + neuron/control FLS) and inflamed (neuron/TNF-FLS + neuron/TNF-FLS media) condition. Comparison made using chi-sq test. * $p < 0.05$. Data from 4-5 female mice in each group. Error bars = SEM.

Additional materials:

- File name: Additional file 1
- File format including the correct file extension: .docx
- Title of data: Table 1, 2 and Figure 1
- Description of data: Table 1 contains list of genes assessed in this study using qPCR and RT-PCR, Table 2 contains location of cytokines detected by the mouse inflammatory antibody array membrane. Figure 1 shows characterization of mouse primary FLS and neuronal activation of FLS secreted MIP-1γ.

References:

1. Bartok B, Firestein GS. Fibroblast-like synoviocytes: key effector cells in rheumatoid arthritis. Immunological reviews. 2010 Jan;233(1):233–255.

2. Bottini N, Firestein GS. Duality of fibroblast-like synoviocytes in RA: passive responders and imprinted aggressors. Nat Rev Rheumatol [Internet]. 2013;9. Available from: http://dx.doi.org/10.1038/nrrheum.2012.190

3. Croft AP, Campos J, Jansen K, Turner JD, Marshall J, Attar M, et al. Distinct fibroblast subsets drive inflammation and damage in arthritis. Nature. 2019 Jun 1;570(7760):246–51.

4. Lee DM, Kiener HP, Agarwal SK, Noss EH, Watts GFM, Chisaka O, et al. Cadherin-11 in Synovial Lining Formation and Pathology in Arthritis. Science. 2007 Feb 16;315(5814):1006.

5. Hardy RS, Hülso C, Liu Y, Gasparini SJ, Fong-Yee C, Tu J, et al. Characterisation of fibroblast-like synoviocytes from a murine model of joint inflammation. Arthritis Research & Therapy. 2013;15(1):R24–R24.

6. von Banchet GS, Richter J, Hückel M, Rose C, Bräuer R, Schaible H-G. Fibroblast-like synovial cells from normal and inflamed knee joints differently affect the expression of pain-related receptors in sensory neurones: a co-culture study. Arthritis Research & Therapy. 2007;9(1):R6–R6.

7. Llop-Guevara A, Porras M, Cendón C, Di Ceglie I, Siracusa F, Madarena F, et al. Simultaneous inhibition of JAK and SYK kinases ameliorates chronic and destructive arthritis in mice. Arthritis Research & Therapy. 2015 Dec 10;17(1):356.

8. Guo W, Yu D, Wang X, Luo C, Chen Y, Lei W, et al. Anti-inflammatory effects of interleukin-23 receptor cytokine-binding homology region rebalance T cell distribution in rodent collagen-induced arthritis. Oncotarget. 2016 May 31;7(22):31800–13.

9. Chen C-X, Chen J-Y, Kou J-Q, Xu Y-L, Wang S-Z, Zhu Q, et al. Suppression of Inflammation and Arthritis by Orally Administrated Cardiotoxin from Naja naja atra. Evid Based Complement Alternat Med. 2015;2015:387094.

10. Hong R, Sur B, Yeom M, Lee B, Kim KS, Rodriguez JP, et al. Anti-inflammatory and anti-arthritic effects of the ethanolic extract of Aralia continentalis Kitag. in IL-1β-stimulated human fibroblast-like synoviocytes and rodent models of polyarthritis and nociception. Phytomedicine. 2018 Jan 1;38:45–56.

773 11. Chakrabarti S, Pattison LA, Singhal K, Hockley JRF, Callejo G, Smith ESJ. Acute
774 inflammation sensitizes knee-innervating sensory neurons and decreases mouse digging
775 behavior in a TRPV1-dependent manner. Neuropharmacology. 2018 Dec 1;143:49–62.

776 12. Woolf CJ, Allchorne A, Safieh-Garabedian B, Poole S. Cytokines, nerve growth factor and
777 inflammatory hyperalgesia: the contribution of tumour necrosis factor α. British Journal of
778 Pharmacology. 1997 May 1;121(3):417–24.

779 13. Andersson SE, Lexmuller K, Johansson A, Ekstrom GM. Tissue and intracellular pH in
780 normal periarticular soft tissue and during different phases of antigen induced arthritis in
781 the rat. J Rheumatol. 1999 Sep;26(9):2018–24.

782 14. Wright AJ, Husson ZMA, Hu D-E, Callejo G, Brindle KM, Smith ESJ. Increased
783 hyperpolarized [1-13C] lactate production in a model of joint inflammation is not
784 accompanied by tissue acidosis as assessed using hyperpolarized 13C-labelled bicarbonate.
785 NMR in Biomedicine. 2018;e3892-n/a.

786 15. Christensen BN, Kochukov M, McNearney TA, Taglialatela G, Westlund KN. Proton-
787 sensing G protein-coupled receptor mobilizes calcium in human synovial cells. Am J
788 Physiol Cell Physiol [Internet]. 2005;289. Available from:
789 http://dx.doi.org/10.1152/ajpcell.00039.2005

790 16. Kolker SJ, Walder RY, Usachev Y, Hillman J, Boyle DL, Firestein GS, et al. Acid-sensing
791 ion channel 3 expressed in type B synoviocytes and chondrocytes modulates hyaluronan
792 expression and release. ANNALS OF THE RHEUMATIC DISEASES. 2010
793 May;69(5):903–9.

794 17. Galindo T, Reyna J, Weyer A. Evidence for Transient Receptor Potential (TRP) Channel
795 Contribution to Arthritis Pain and Pathogenesis. Pharmaceuticals (Basel, Switzerland).
796 2018 Oct 15;11(4):105.

797 18. Kochukov MY, McNearney TA, Fu Y, Westlund KN. Thermosensitive TRP ion channels
798 mediate cytosolic calcium response in human synoviocytes. Am J Physiol Cell Physiol
799 [Internet]. 2006;291. Available from: http://dx.doi.org/10.1152/ajpcell.00553.2005

800 19. Itoh Y, Hatano N, Hayashi H, Onozaki K, Miyazawa K, Muraki K. An environmental
801 sensor, TRPV4 is a novel regulator of intracellular Ca2+ in human synoviocytes. American
802 Journal of Physiology-Cell Physiology. 2009 Sep 16;297(5):C1082–90.

803 20. Kochukov MY, McNearney TA, Yin H, Zhang L, Ma F, Ponomareva L, et al. Tumor
804 Necrosis Factor-Alpha (TNF-α) Enhances Functional Thermal and Chemical Responses of
805 TRP Cation Channels in Human Synoviocytes. Mol Pain. 2009 Jan 1;5:1744-8069-5–49.

806 21. Sluka KA, Rasmussen LA, Edgar MM, O'Donnell JM, Walder RY, Kolker SJ, et al. Acid-
807 sensing ion channel 3 deficiency increases inflammation but decreases pain behavior in
808 murine arthritis. 2013;(1529-0131 (Electronic)).

809 22. Gong W, Kolker SJ, Usachev Y, Walder RY, Boyle DL, Firestein GS, et al. Acid-sensing
810 ion channel 3 decreases phosphorylation of extracellular signal-regulated kinases and
811 induces synoviocyte cell death by increasing intracellular calcium. Arthritis Research &
812 Therapy. 2014;16(3):R121.

813 23. Lebre MC, Vieira PL, Tang MW, Aarrass S, Helder B, Newsom-Davis T, et al. Synovial
814 IL-21/TNF-producing CD4+ T cells induce joint destruction in rheumatoid arthritis by
815 inducing matrix metalloproteinase production by fibroblast-like synoviocytes. Journal of
816 Leukocyte Biology. 2017 Mar 1;101(3):775–83.

817 24. Bombara MR, Webb DL, Conrad P, Marior CW, Sarr T, Ranges GE, et al. Cell contact
818 between T cells and synovial fibroblasts causes induction of adhesion molecules and
819 cytokines. Journal of Leukocyte Biology. 1993 Nov 1;54(5):399–406.

820 25. Yamamura Y, Gupta R, Morita Y, He X, Pai R, Endres J, et al. Effector Function of Resting
821 T Cells: Activation of Synovial Fibroblasts. J Immunol. 2001 Feb 15;166(4):2270.

822 26. Burger D, Rezzonico R, Li J-M, Modoux C, Pierce RA, Welgus HG, et al. Imbalance
823 between interstitial collagenase and tissue inhibitor of metalloproteinases 1 in synoviocytes
824 and fibroblasts upon direct contact with stimulated T lymphocytes: Involvement of
825 membrane-associated cytokines. Arthritis & Rheumatism. 1998 Oct 1;41(10):1748–59.

826 27. Bondeson J, Wainwright SD, Lauder S, Amos N, Hughes CE. The role of synovial
827 macrophages and macrophage-produced cytokines in driving aggrecanases, matrix
828 metalloproteinases, and other destructive and inflammatory responses in osteoarthritis.
829 Arthritis Research & Therapy. 2006 Dec 19;8(6):R187.

830 28. Blue ML, Conrad P, Webb DL, Sarr T, Macaro M. Interacting monocytes and synoviocytes
831 induce adhesion molecules by a cytokine-regulated process. Lymphokine Cytokine Res.
832 1993 Aug;12(4):213–8.

833 29. Chomarat P, Rissoan MC, Pin JJ, Banchereau J, Miossec P. Contribution of IL-1, CD14,
834 and CD13 in the increased IL-6 production induced by in vitro monocyte-synoviocyte
835 interactions. J Immunol. 1995 Oct 1;155(7):3645.

836 30. Scott BB, Weisbrot LM, Greenwood JD, Bogoch ER, Paige CJ, Keystone EC. Rheumatoid
837 arthritis synovial fibroblast and U937 macrophage/monocyte cell line interaction in
838 cartilage degradation. Arthritis & Rheumatism. 1997 Mar 1;40(3):490–8.

839 31. Benito-Miguel M, García-Carmona Y, Balsa A, Bautista-Caro M-B, Arroyo-Villa I, Cobo-
840 Ibáñez T, et al. IL-15 Expression on RA Synovial Fibroblasts Promotes B Cell Survival.
841 PLOS ONE. 2012 Jul 9;7(7):e40620.

842 32. Chan A, Filer A, Parsonage G, Kollnberger S, Gundle R, Buckley CD, et al. Mediation of
843 the proinflammatory cytokine response in rheumatoid arthritis and spondylarthritis by
844 interactions between fibroblast-like synoviocytes and natural killer cells. Arthritis &
845 Rheumatism. 2008 Mar 1;58(3):707–17.

846 33. Chakrabarti S, Jadon DR, Bulmer DC, Smith ESJ. Human osteoarthritic synovial fluid
847 increases excitability of mouse dorsal root ganglion sensory neurons: an in-vitro
848 translational model to study arthritic pain. Rheumatology [Internet]. 2019 Aug 13 [cited
849 2019 Aug 14]; Available from: https://doi.org/10.1093/rheumatology/kez331

850 34. Hannan MT. Epidemiologic perspectives on women and arthritis: An overview. Arthritis &
851 Rheumatism. 1996 Dec 1;9(6):424–34.

852 35. Futami I, Ishijima M, Kaneko H, Tsuji K, Ichikawa-Tomikawa N, Sadatsuki R, et al.
853 Isolation and Characterization of Multipotential Mesenchymal Cells from the Mouse
854 Synovium. PLoS ONE. 2012 Sep 18;7(9):e45517.

855 36. McCall MN, McMurray HR, Land H, Almudevar A. On non-detects in qPCR data.
856 Bioinformatics. 2014 Aug 15;30(16):2310–6.

857 37. Livak KJ, Schmittgen TD. Analysis of Relative Gene Expression Data Using Real-Time
858 Quantitative PCR and the 2−ΔΔCT Method. Methods. 2001 Dec 1;25(4):402–8.

859 38. Stefanini M, Martino C de, Zamboni L. Fixation of Ejaculated Spermatozoa for Electron
860 Microscopy. Nature. 1967 Oct 1;216(5111):173–4.

861 39. Dittert I, Benedikt J, Vyklický L, Zimmermann K, Reeh PW, Vlachová V. Improved
862 superfusion technique for rapid cooling or heating of cultured cells under patch-clamp
863 conditions. Journal of Neuroscience Methods. 2006 Mar 15;151(2):178–85.

864 40. Elizur A, Adair-Kirk TL, Kelley DG, Griffin GL, Demello DE, Senior RM. Tumor necrosis
865 factor-alpha from macrophages enhances LPS-induced clara cell expression of
866 keratinocyte-derived chemokine. Am J Respir Cell Mol Biol. 2008 Jan;38(1):8–15.

867 41. Rojewska E, Zychowska M, Piotrowska A, Kreiner G, Nalepa I, Mika J. Involvement of
868 Macrophage Inflammatory Protein-1 Family Members in the Development of Diabetic
869 Neuropathy and Their Contribution to Effectiveness of Morphine. Front Immunol. 2018
870 Mar 12;9:494–494.

871 42. Dawes JM, Kiesewetter H, Perkins JR, Bennett DLH, McMahon SB. Chemokine
872 expression in peripheral tissues from the monosodium iodoacetate model of chronic joint
873 pain. Mol Pain. 2013 Nov 8;9:57–57.

874 43. Syx D, Tran PB, Miller RE, Malfait A-M. Peripheral Mechanisms Contributing to
875 Osteoarthritis Pain. Current Rheumatology Reports. 2018 Feb 26;20(2):9.

876 44. Rosengren S, Boyle DL, Firestein GS. Acquisition, culture, and phenotyping of synovial
877 fibroblasts. Methods in molecular medicine. 2007;135:365–375.

878 45. Ai R, Hammaker D, Boyle DL, Morgan R, Walsh AM, Fan S, et al. Joint-specific DNA
879 methylation and transcriptome signatures in rheumatoid arthritis identify distinct
880 pathogenic processes. Nat Commun. 2016 Jun 10;7:11849–11849.

881 46. Kawashima M, Ogura N, Akutsu M, Ito K, Kondoh T. The anti-inflammatory effect of
882 cyclooxygenase inhibitors in fibroblast-like synoviocytes from the human
883 temporomandibular joint results from the suppression of PGE2 production. Journal of oral
884 pathology & medicine : official publication of the International Association of Oral
885 Pathologists and the American Academy of Oral Pathology. 2013 Jul;42(6):499–506.

886 47. Larsson S, Englund M, Struglics A, Lohmander LS. Interleukin-6 and tumor necrosis factor
887 alpha in synovial fluid are associated with progression of radiographic knee osteoarthritis in
888 subjects with previous meniscectomy. Osteoarthritis and Cartilage. 2015 Nov
889 1;23(11):1906–14.

890 48. Tetta C, Camussi G, Modena V, Di Vittorio C, Baglioni C. Tumour necrosis factor in serum
891 and synovial fluid of patients with active and severe rheumatoid arthritis. Ann Rheum Dis.
892 1990 Sep;49(9):665–7.

893 49. Parsonage G, Falciani F, Burman A, Filer A, Ross E, Bofill M, et al. Global gene
894 expression profiles in fibroblasts from synovial, skin and lymphoid tissue reveals distinct
895 cytokine and chemokine expression patterns. Thromb Haemost. 2017 May 12;90(10):688–
896 97.

897 50. Taylor PC, Feldmann M. Anti-TNF biologic agents: still the therapy of choice for
898 rheumatoid arthritis. Nature Reviews Rheumatology. 2009 Oct 1;5:578.

899 51. Jones DS, Jenney AP, Swantek JL, Burke JM, Lauffenburger DA, Sorger PK. Profiling
900 drugs for rheumatoid arthritis that inhibit synovial fibroblast activation. Nature Chemical
901 Biology. 2016 Oct 31;13:38.

902 52. Pattison LA, Callejo G, St John Smith E. Evolution of acid nociception: ion channels and
903 receptors for detecting acid. Philosophical Transactions of the Royal Society B: Biological
904 Sciences. 2019 Nov 11;374(1785):20190291.

905 53. Akopian AN, Ruparel NB, Jeske NA, Hargreaves KM. Transient receptor potential TRPA1
906 channel desensitization in sensory neurons is agonist dependent and regulated by TRPV1-
907 directed internalization. J Physiol. 2007 Aug 15;583(Pt 1):175–93.

908 54. Wang YY, Chang RB, Waters HN, McKemy DD, Liman ER. The nociceptor ion channel
909 TRPA1 is potentiated and inactivated by permeating calcium ions. J Biol Chem. 2008 Nov
910 21;283(47):32691–703.

911 55. Sarria I, Ling J, Zhu MX, Gu JG. TRPM8 acute desensitization is mediated by calmodulin
912 and requires PIP(2): distinction from tachyphylaxis. J Neurophysiol. 2011
913 Dec;106(6):3056–66.

914 56. Czeschik JC, Hagenacker T, Schäfers M, Büsselberg D. TNF-α differentially modulates ion
915 channels of nociceptive neurons. Neuroscience Letters. 2008 Apr 4;434(3):293–8.

916 57. Miller RJ, Jung H, Bhangoo SK, White FA. Cytokine and chemokine regulation of sensory
917 neuron function. Handb Exp Pharmacol. 2009;(194):417–49.

58. Schaible H-G. Nociceptive neurons detect cytokines in arthritis. ARTHRITIS RESEARCH & THERAPY. 2014;16(5).

59. Fang D, Kong L-Y, Cai J, Li S, Liu X-D, Han J-S, et al. Interleukin-6-mediated functional upregulation of TRPV1 receptors in dorsal root ganglion neurons through the activation of JAK/PI3K signaling pathway: roles in the development of bone cancer pain in a rat model. Pain. 2015 Jun;156(6):1124–44.

60. Brandolini L, Benedetti E, Ruffini PA, Russo R, Cristiano L, Antonosante A, et al. CXCR1/2 pathways in paclitaxel-induced neuropathic pain. Oncotarget. 2017 Apr 4;8(14):23188–201.

61. Oh SB, Tran PB, Gillard SE, Hurley RW, Hammond DL, Miller RJ. Chemokines and Glycoprotein120 Produce Pain Hypersensitivity by Directly Exciting Primary Nociceptive Neurons. J Neurosci. 2001 Jul 15;21(14):5027.

62. Donatien P, Anand U, Yiangou Y, Sinisi M, Fox M, MacQuillan A, et al. Granulocyte-macrophage colony-stimulating factor receptor expression in clinical pain disorder tissues and role in neuronal sensitization. Pain Rep. 2018 Sep 17;3(5):e676–e676.

63. Merabova N, Kaminski R, Krynska B, Amini S, Khalili K, Darbinyan A. JCV agnoprotein-induced reduction in CXCL5/LIX secretion by oligodendrocytes is associated with activation of apoptotic signaling in neurons. J Cell Physiol. 2012 Aug;227(8):3119–27.

64. Jung H, Toth PT, White FA, Miller RJ. Monocyte chemoattractant protein-1 functions as a neuromodulator in dorsal root ganglia neurons. J Neurochem. 2008 Jan;104(1):254–63.

65. Gowler PRW, Li L, Woodhams SG, Bennett AJ, Suzuki R, Walsh DA, et al. Peripheral brain derived neurotrophic factor contributes to chronic osteoarthritis joint pain. PAIN [Internet]. 2019;Articles in Press. Available from: https://journals.lww.com/pain/Fulltext/publishahead/Peripheral_brain_derived_neurotrophic_factor.98598.aspx

66. Neogi T. The epidemiology and impact of pain in osteoarthritis. Osteoarthritis and Cartilage. 2013 Sep 1;21(9):1145–53.

950

951

952

953

954

955

956

957

958 Table 1: AP properties of knee neurons. *** represents $p < 0.001$ when compared to knee neuron

959 mono-culture, $ represents $p < 0.05$ when compared to neuron/control FLS co-culture.

	Knee neuron mono-culture (n = 19)		Knee neuron/control FLS (n = 18)		Knee neuron/TNF-FLS (n = 21)		Knee neuron/TNF-FLS media (n = 20)	
	Mean	SEM	Mean	SEM	Mean	SEM	Mean	SEM.
RMP (mV)	-46.6	2.0	-42.8	2.9	-39.7	2.3	-32.0***/$	2.3
Threshold (pA)	447.4	71.5	319.4	56.3	245.2	49.4	315.0	70.0
Half peak duration (HPD, ms)	2.2	0.4	2.3	0.2	2.4	0.5	2.4	0.6
Afterhyperpolarization amplitude (AHP peak, mV)	13.7	2.6	19.6	2.7	16.1	2.9	21.6	3.3

Figure 1

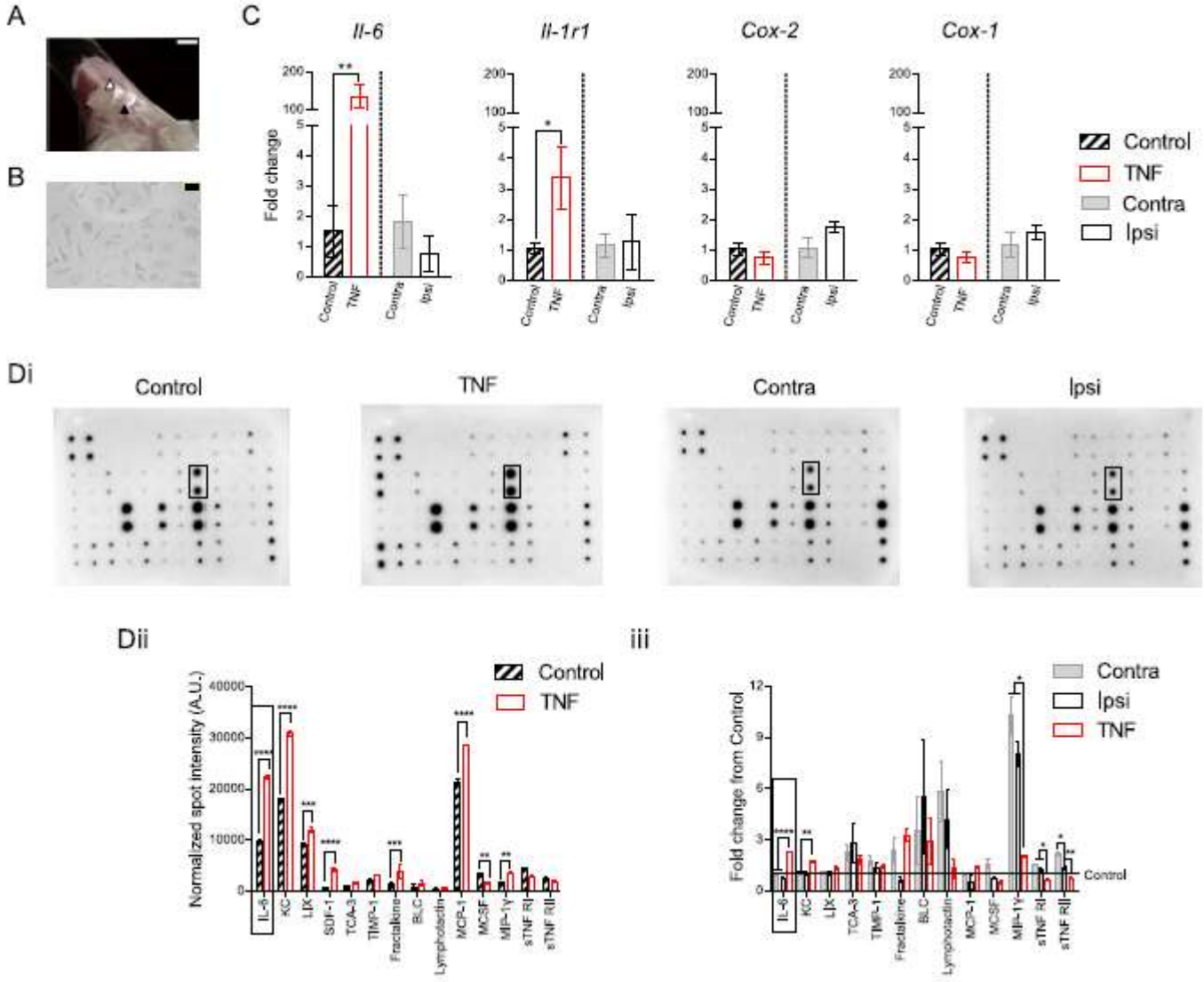

967

968

969

970

971

972

973

Figure 2

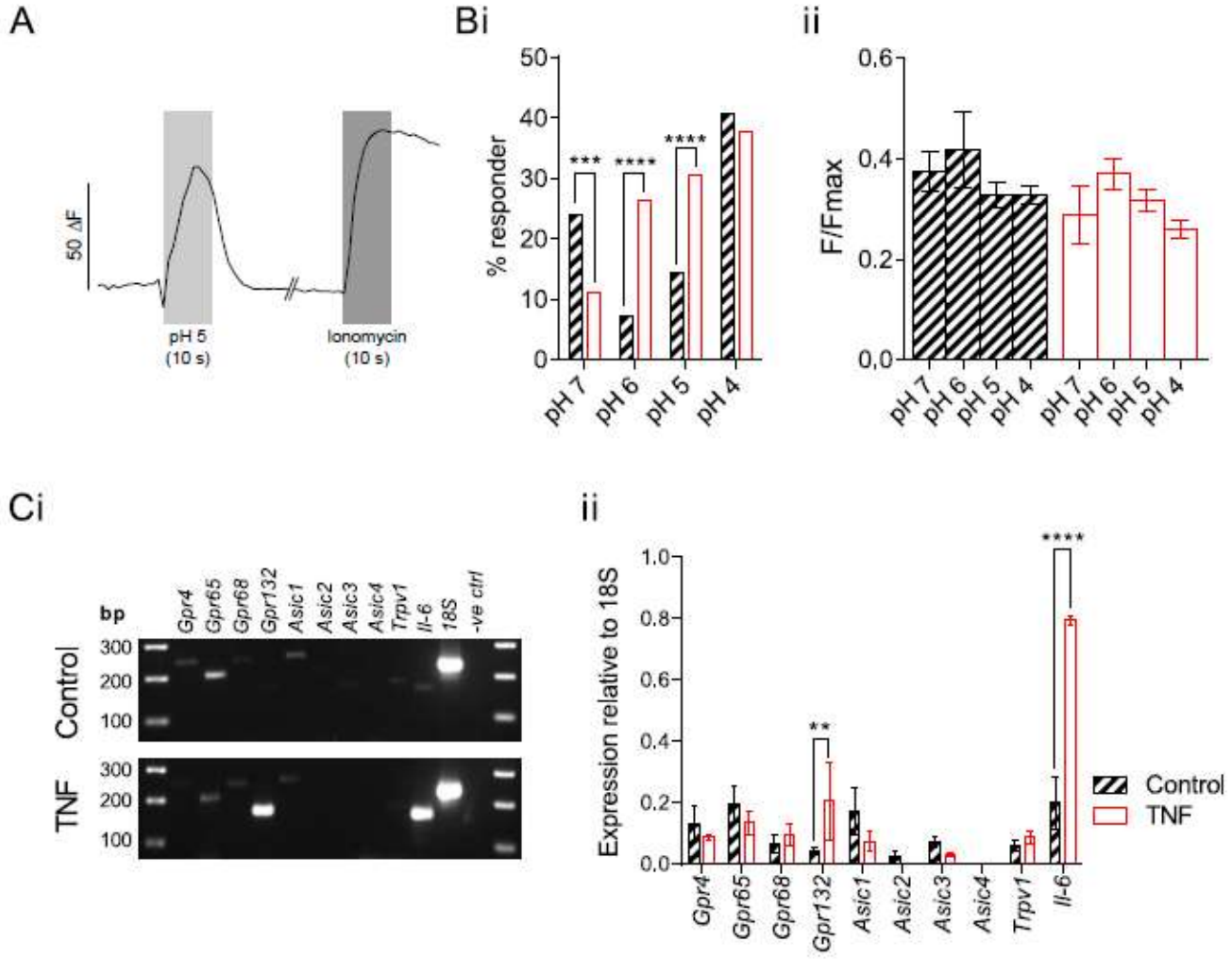

974

975

976

977

978

979

980

981

Figure 3

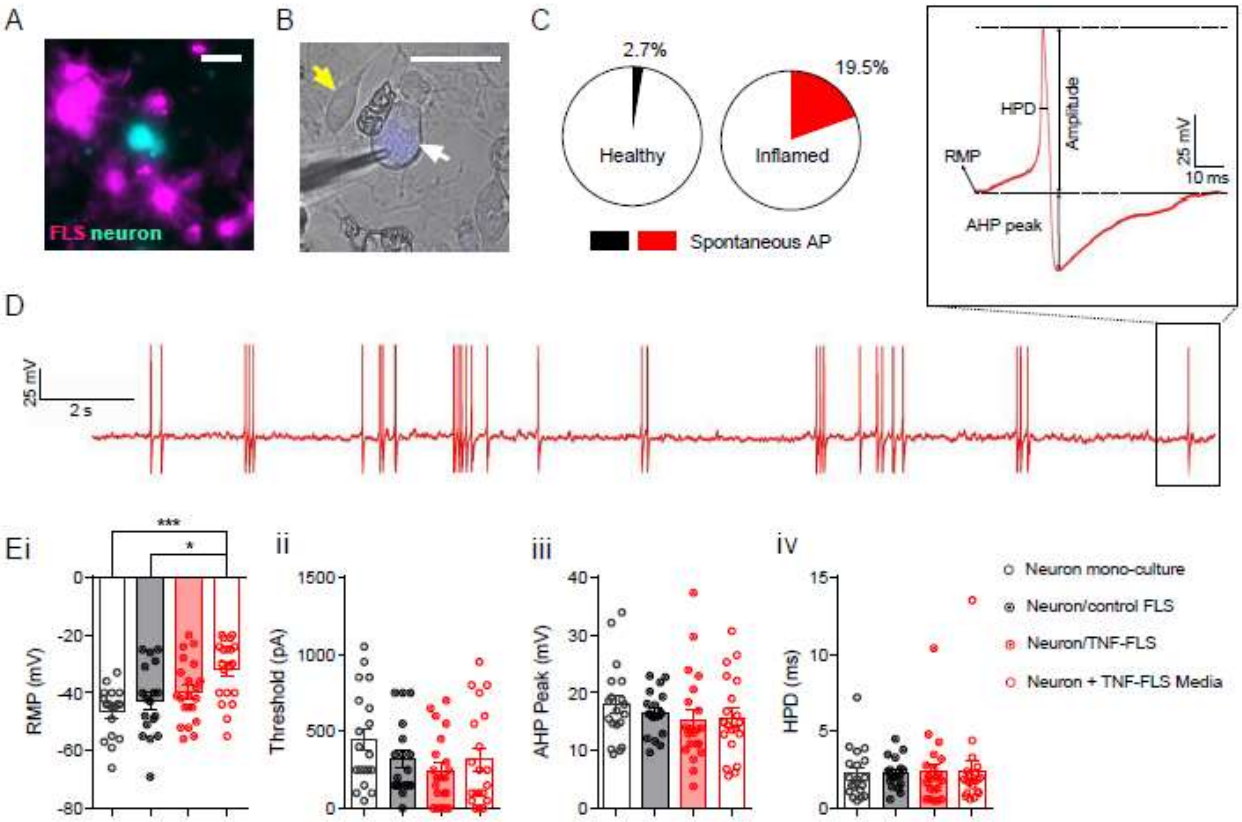

982

983

984

985

986

987

988

989

990

991

Figure 4

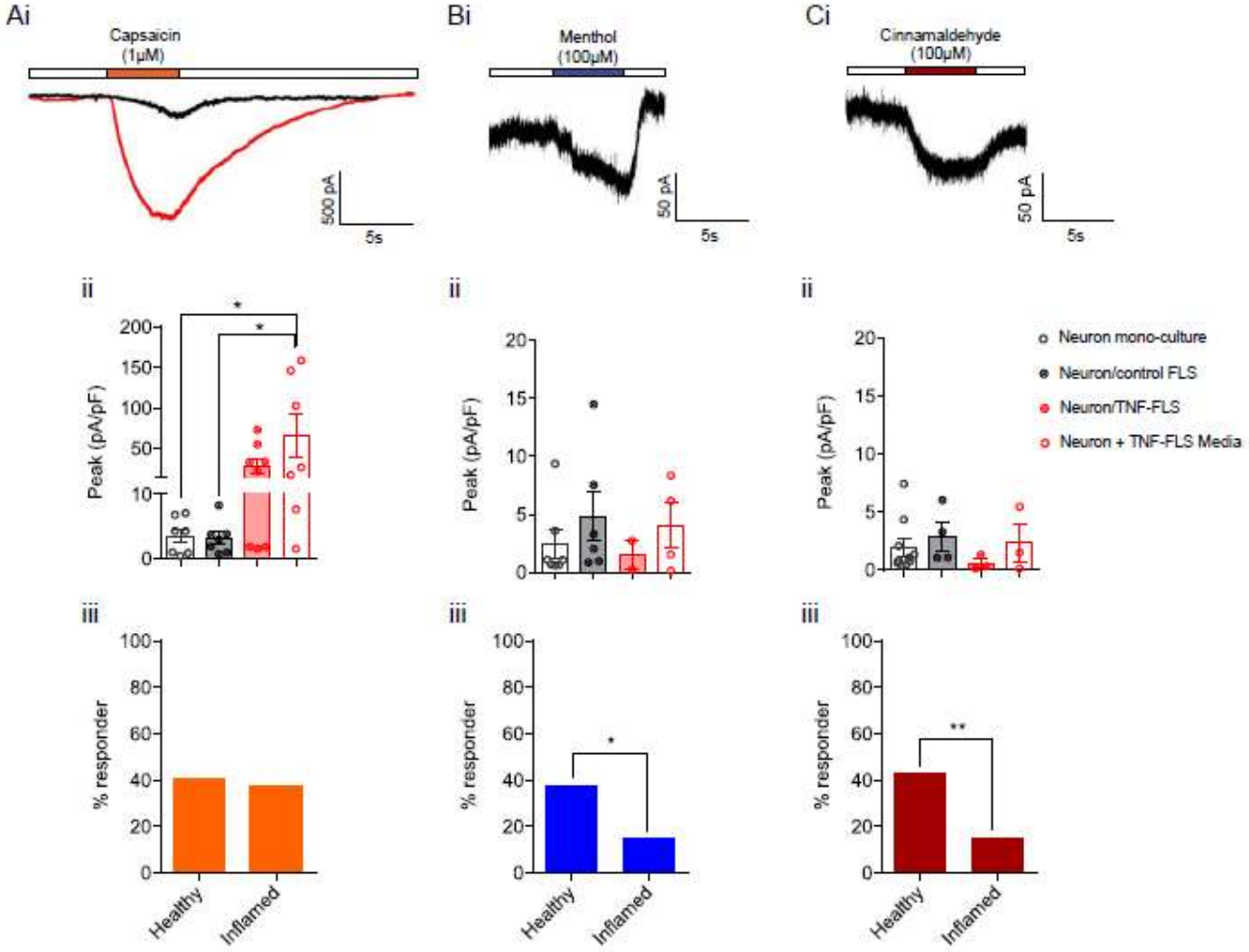

992

993

994

995

996

997

998

999

1000 Supplementary Table 1: Genes of interest analyzed in this study.

Gene	TaqMan Assay ID/sequence	Role
Taqman Probes		
18S	Mm03928990_g1	Housekeeping
Cd-68	Mm03047343_m1	Macrophage marker
Cdh-11	Mm00515466_m1	Intimal synovial fibroblast marker
Cd-248	Mm00547485_s1	Synovial fibroblast marker
Cd-31	Mm01242576_m1	Endothelial marker
Il-6	Mm00446190_m1	Inflammation
Il-1r1	Mm00434237_m1	Inflammation
Cox-1	Mm04225243_g1	Constitutively active gene
Cox-2	Mm03294838_g1	Inflammation
RT-PCR primers		
18S	Fwd: CCGGTACAGTGAAACTGCGA Rev: ATCTAGAGTCACCAAGCCGC Product size: 230 bp	Housekeeping
Gpr4	Fwd: ATTCAGCACCGCTCTTCCAT Rev: CAGGGCCAGACGTTTGATCT Product size: 236 bp	Proton-sensing GPCR
Gpr65	Fwd: CAACATCGGATCTTTATGCG Rev: ATGTAGGTGAAGAAAACGCT Product size: 195 bp	Proton-sensing GPCR
Gpr68	Fwd: TTCTCCCTCCTCCTCACCAG Rev: GGCTGAGTGGAGCTTGGTTA Product size: 234 bp	Proton-sensing GPCR
Gpr132	Fwd: CCACTACCTGCGTTTCACCT Rev: CCAGGAAGATGGTGACGACC Product size: 161 bp	Proton-sensing GPCR
Asic1	Fwd: ACACATTCAACTCGGGCCAA Rev: TGCTCCTGGCAAGACACAAA Product size: 250 bp	Acid-sensing ion channel

Asic2	Fwd: TGCTGCCTTACTTGGTGACA Rev: CGGAGTGGTTTGGCATTGTG Product size: 194 bp	Acid-sensing ion channel
Asic3	Fwd: AGAAGGAGCTCTCAAAGGCG Rev: AGGTAACAGGTACGGTGGGA Product size: 158 bp	Acid-sensing ion channel
Asic4	Fwd: AGCGGCTAACTTATCTGCCC Rev: CAAGGGAGTCCAGTGTGTGG Product size: 234 bp	Acid-sensing ion channel
Trpv1	Fwd: GACACCATTGCTCTGCTCCT Rev: GCCTGGACATCTGCTCCATT Product size: 176 bp	Heat and proton transducing ion channel
Il6	Fwd: AGCCAGAGTCCTTCAGAGAGA Rev: TGGTCTTGGTCCTTAGCCAC Product size: 226 bp	Inflammation

Fwd = Forward primer sequence, Rev = reverse primer sequence.

1013 Supplementary Table 2: Location of cytokines detected by the mouse inflammatory antibody

1014 array membrane.

	A	B	C	D	E	F	G	H	I	J	K	L
1	Pos	Pos	Neg	Neg	Blank	BLC	CD30 L	Eotaxin	Eotaxin-2	Fas Ligand	Fractalkine	GCSF
2	Pos	Pos	Neg	Neg	Blank	BLC	CD30 L	Eotaxin	Eotaxin-2	Fas Ligand	Fractalkine	GCSF
3	GM-CSF	IFNγ	IL-1α	IL-1β	IL-2	IL-7	IL-4	IL-6	IL-9	IL-10	IL-12 p40/p70	IL-12 p70
4	GM-CSF	IFNγ	IL-1α	IL-1β	IL-2	IL-7	IL-4	IL-6	IL-9	IL-10	IL-12 p40/p70	IL-12 p70
5	IL-13	IL-17	I-TAC	KC	Leptin	LIX	Lymphotactin	MCP-1	MCSF	MIG	MIP-1α	MIP-1γ
6	IL-13	IL-17	I-TAC	KC	Leptin	LIX	Lymphotactin	MCP-1	MCSF	MIG	MIP-1α	MIP-1γ
7	RANTES	SDF-1	TCA-3	TECK	TIMP-1	TIMP-2	TNF-α	sTNF RI	sTNF RII	Blank	Blank	Pos
8	RANTES	SDF-1	TCA-3	TECK	TIMP-1	TIMP-2	TNF-α	sTNF RI	sTNF RII	Blank	Blank	Pos

1015

1016 BLC = B lymphocyte chemoattractant, GCSF = granulocyte colony stimulating factor, GM-CSF

1017 = granulocyte-macrophage colony stimulating factor, IFN = interferon, IL= interleukin, I-TAC =

1018 interferon inducible T-cell alpha chemoattractant, KC = Keratinocyte chemoattractant (chemokine

1019 ligand 1), LIX = lipopolysaccharide induced chemokine, MCP = monocyte chemoattractant

1020 protein, MCSF = macrophage colony stimulating factor, MIG = monokine induced by gamma

1021 interferon, MIP = macrophage inflammatory protein, RANTES = Regulated on activation, normal

1022 T-cell expressed and secreted, SDF= stromal cell derived factor, TCA = T-cell activation gene,

1023 TECK = thymus expressed chemokine, TIMP = Tissue inhibitor of metalloproteinase, TNF(R) =

1024 tumor necrosis factor (receptor), Pos = Positive spot, Neg = negative spot.

1025

1026

Supplementary Figure 1

Characterization of FLS

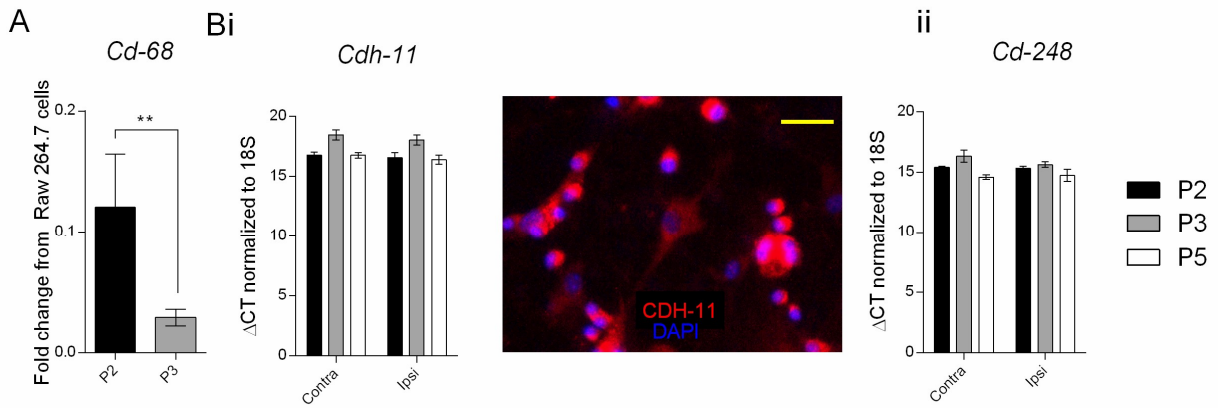

Expression of inflammation-related genes in FLS derived from CFA-injected knee joint

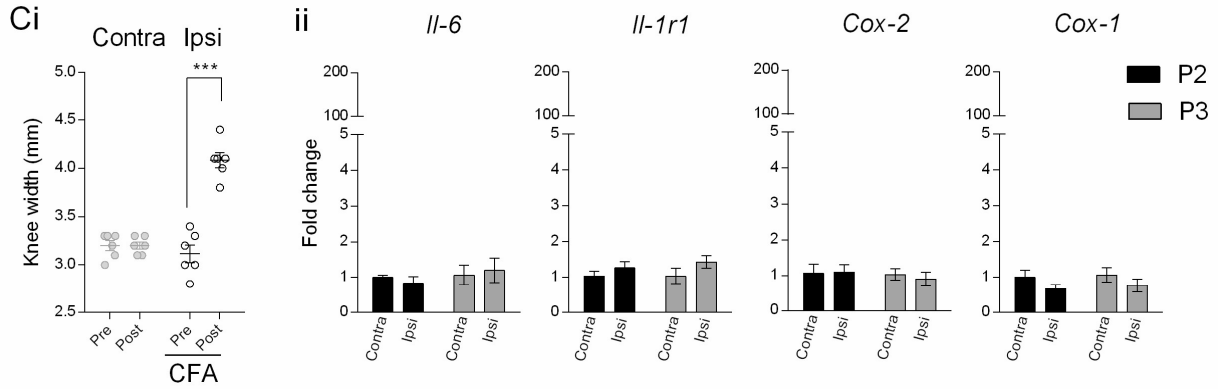

MIP-1γ activation of DRG neurons

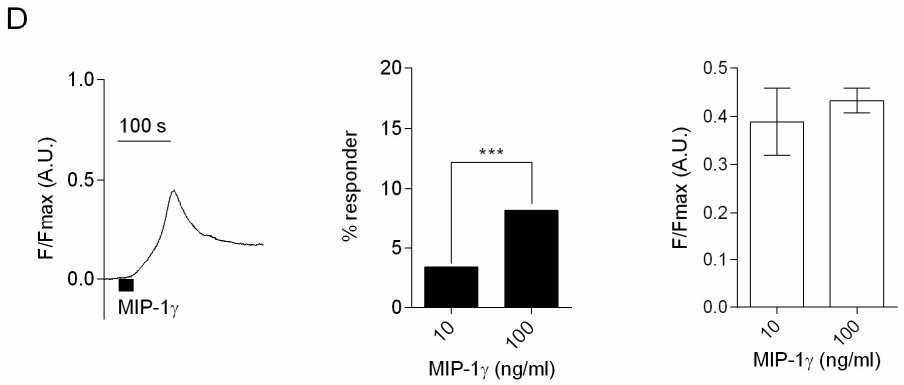

1027

1028

1029

1030 Supplementary Figure 1: Characterization of mouse primary FLS and neuronal activation of FLS
1031 secreted MIP-1γ. A) Bars showing reduction in mRNA expression of the macrophage marker *Cd-*
1032 *68* from P2 to P3 expressed as fold change from macrophage cell line Raw 264.7 cells. ** $p < 0.01$,
1033 ratio paired t-test. Bi) Expression of FLS marker *Cdh-11* across P2-P5 in ipsi and contra FLS
1034 normalized to housekeeping gene *18S* (left) and a representative image of CDH-11 (red) and DAPI
1035 (blue) stained FLS in culture. ii) Expression of FLS marker *Cd-68* across P2-P5 in ipsi and contra
1036 FLS normalized to housekeeping gene *18S*. Ci) Mouse knee width in Contra (grey circles) and Ipsi
1037 (open circles) limbs before and after injection of CFA (n = 6, paired t-test. ii) Bars represent fold
1038 change of the genes *Il-6*, *Il-1r1*, *Cox-2* and *Cox-1* from Contra vs. Ipsi. Black bars = P2, grey bars
1039 = P3. D) Intracellular Ca^{2+} influx in lumbar DRG neurons in response to 20 s application of 100
1040 ng/ml MIP-1γ, followed by percentage of neurons responding to 10 and 100 ng/ml of MIP-1γ and
1041 their respective peak response. > 500 neurons imaged from three male mice. *** $p < 0.001$, chi-
1042 sq test. Error bars represent SEM.

1043

1044

1045